Supporting information for

Intrinsic Self-Trapped Broadband Emission from Zinc Halide-Based Metal-Organic Frameworks

Wen Ma, [a] Xueling Song, [a] Jinlin Yin, [a] & Honghan Fei [a], *

[a]School of Chemical Science and Engineering, Shanghai Key Laboratory of Chemical Assessment and Sustainability, Tongji University, Shanghai 200092, P. R. China

Corresponding Author

fei@tongji.edu.cn

Experimental Section

Materials

ZnCl$_2$ (98.0%, TCI), ZnBr$_2$ (98%, TCI), ZnI$_2$ (98%, Sigma-Aldrich), 1-chloro-2,4-dinitrobenzene (99%, TCI), Catechol (99%, Sigma-Aldrich), K$_2$CO3 (99%, Sigma-Aldrich), Fuming HNO$_3$ (AR, SCR), H$_2$SO$_4$ (95-98%, SCR), HCl (36-38%, SCR), Sn Powder (99.5%, Sigma-Aldrich), NaNO$_2$ (98%, Alfa Aesar), Acetic Acid (99%, Adamas), Tris-(8-hydroxyquinoline)aluminum (Alq3, 98%, TCI), Methanol (MeOH, 99.5%, Greagent), N,N-dimethylformamide (99.5%, Greagent), Ethanol (99.7%, Greagent), Dichloromethane (DCM, 99.5%, Greagent) and ethanol (EtOH, 99.7%, Greagent) were used as received without further purification. Deionized water was obtained from a BARNSTEAD PACIFIC RO water purification system.

Synthesis of H$_2$BTDD

H$_2$BTDD was synthesized with slight modification of the previous literature[S1] according to the following scheme:
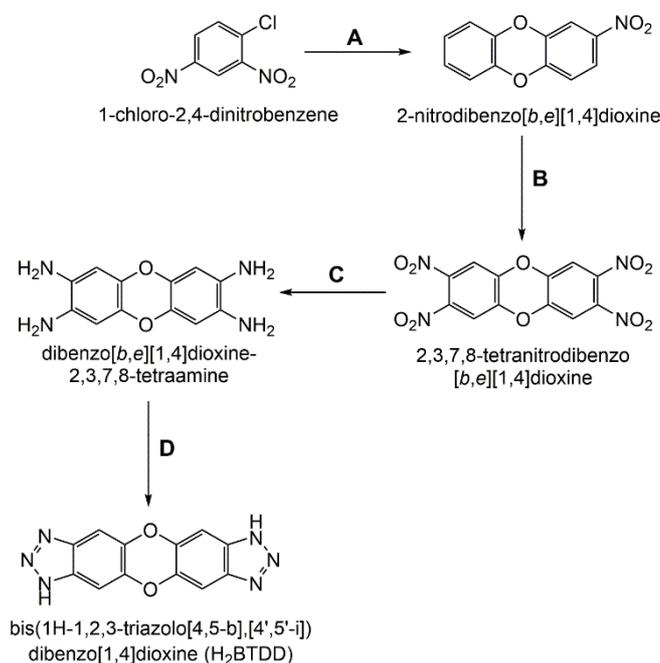
Scheme S1. Synthesis pathway to H$_2$BTDD.

Reaction A. 30.02 g potassium carbonate was dissolved in 120 mL N,N-dimethylformamide (DMF) in a 250 mL round bottom flask under N$_2$ atmosphere. To the stirring solution was then

added 11.9 g catechol and 20 g 1-chloro-2,4-dinitrobenzene. The mixture was heated to 60 °C with reflux overnight and cooled to room temperature, after which the yellow solids were poured into 250 mL ice water, filtered and washed with deionized water for several times. The yellow product was dissolved in 1 L hot acetone, which was cooled to room temperature and 400 mL DI water was slowly added. The resulting light yellow solids were filtered, washed with DI water (20 mL×3), and dried under vacuum to obtain 2-nitrodibenzo[b,e][1,4]dioxin. Yield: 22.4 g (99%). ^{1}H NMR (600 MHz, d^6-DMSO) δ 7.90 (d, 1H), 7.80 (s, 1H), 7.20 (d, 1H), 7.06 (d, 2H), 7.05 (d, 2H).

Reaction B. In 500 mL round bottom flask, 10 g 2-nitrodibenzo[b,e][1,4]dioxin was added into 45 mL fuming HNO_3 in portions, then 15 mL H_2SO_4 was introduced to the stirring solution from the top of reflux by dripping slowly. Using ice bath to control the reaction temperature lower than 10 °C. Subsequently, the mixture was heated to 70 °C with reflux overnight and cooled to room temperature. The yellow product was filtered, washed with DI water (20 mL×3), and dried under vacuum to obtain 2,3,7,8-tetranitrodibenzo[b,e][1,4]dioxine. Yield: 9.52 g (60%). ^{1}H NMR (600 MHz, d^6-DMSO) δ 8.03 (s, 4H).

Reaction C. 7.2 g 2,3,7,8-tetranitrodibenzo[b,e][1,4]dioxine was dissolved into 125 mL HCl solutions in a 250 mL beaker, then 30 g Sn powder was added into stirring solutions with portions. After 30 minutes standing, the yellow precipitates were turned into pale white. The mixture was transferred into a 500 mL RFB, and added to 50 °C with reflux for 8 h. Next, the RFB was cooled down in ice bath with white precipitates. The product was filtered, washed with HCl (5 mL×3), EtOH (20 mL×3) and EtAc (20 mL×3), then dried under vacuum to obtain dibenzo[b,e][1,4]dioxine-2,3,7,8-tetraamine. Yield: 7.21 g (79%). ^{1}H NMR (600 MHz, d^4-CD$_3$OD) δ 6.62 (s, 4H).

Reaction D. In an ice bath, 1.6 g dibenzo[b,e][1,4]dioxine-2,3,7,8-tetraamine, 15 mL CH_3COOH, 2 mL DI water was added into a 250 mL RFB with stirring. 2.5 mL $NaNO_2$ aqueous (2.75 g $NaNO_2$ dissolved in 10 mL DI water) was dripped in 2.5 minutes, while the white mixture was turned into dark green, orange and brown finally. The reaction remained 30 minutes below 10 °C and 50 mL DI water was added. The mixture was filtered, washed with DI water (20 mL×3) and

CH$_3$OH (20 mL × 3), and dried under vacuum to obtain bis(1H-1,2,3-triazolo[4,5-b],[4′,5′-i])dibenzo[1,4]dioxin (H$_2$BTDD). Yield: 0.95 g (74%). ^{1}H NMR (600 MHz, d^4-CF$_3$COOD) δ 7.66 (s, 4H).

Solvothermal Synthesis of MFU-4l(Zn)-X (X = Cl, Br, I)

In a typical synthesis[S2], 200 mg H$_2$BTDD was added into 200 mL N-N-dimethylformamide (DMF) in a 500 mL round bottom flask with stirring. The mixture was heating to 130 C° under reflux until all the solids dissolved, and then cooled down to the room temperature. Subsequently, 15 mmol anhydrous ZnX$_2$ (20 eq. based on Zn) was introduced under stirring, after that the mixture was heated to 145 °C for 24 h with reflux. After 24 h, the product was cooled down to room temperature and the powders were isolated by filtered, washed with DMF and MeOH, and dried in air at 70 °C. Anal. cal. for C$_{36}$H$_{12}$N$_{18}$Cl$_4$Zn$_5$: C 37.14, H 1.03, N 21.67 (%); found: C 37.19, H 1.07, N 21.69 (%, activated sample). Anal. cal. for C$_{36}$H$_{12}$N$_{18}$Br$_4$Zn$_5$: C 32.21, H 0.89, N 18.79 (%); found: C 32.15, H 0.88, N 18.74 (%, activated sample). Anal. cal. for C$_{36}$H$_{12}$N$_{18}$I$_4$Zn$_5$: C 28.25, H 0.78, N 16.48 (%); found: C 28.22, H 0.74, N 16.45 (%, activated sample).

Synthesis of Alq3@MFU-4l(Zn)-Br

The samples of Zn$_5$Br$_4$BTDD$_3$ (40 mg) were dipped in 10 ml DMF solutions containing Alq3 (1×10^{-3} mol L^{-1}) under stirring in 10 ml sealed glass bottles. After 0.5, 1, 1.5, 2 and 3 hours, the immersed samples were taken out and washed with DMF (10 mL×5) and MeOH (10 mL×5) to remove residual Alq3 complex on the surface. The powders were collected by filtered and dried in air at 70 °C. Inductively coupled plasma optical emission spectra (ICP-OES, operated on a PERKIN ELMER AVIO 200 ICP-OES spectrometer) was employed to evidence the successful incorporation of Alq3 into Zn$_5$Br$_4$BTDD$_3$ (based on Al).

Nuclear Magnetic Resonance (NMR) Spectra

Nuclear magnetic resonance (NMR) spectra were carried out on a AVANCE III HD spectrometer (600 MHz); chemical shifts were quoted in parts per million (ppm) referenced to the appropriate solvent peak or 0 ppm for tetramethylsilane (TMS).

Element Analysis (EA)

Elemental analysis (EA) for C/H/N/S was performed in a Varian EL III element analyzer.

Powder X-ray Diffraction (PXRD)

Powder X-ray Diffraction (PXRD) analysis was performed using on a BRUKER D2 PHASER X-ray diffractometer equipped with a Cu sealed tube (λ = 1.54184 Å) at 30 kV and 10 mA. The diffraction patterns were scanned at ambient temperature, with a scan speed of 1 sec/step, a step size of 0.02 ° in 2θ, and a 2θ range of 3.5 ~ 40 °. Simulated powder patterns were calculated by Mercury software using the crystallographic information file from the Cambridge Crystallographic Data Center.

Fourier-transform Infrared (FT-IR) Spectrum

FT-IR spectrum were recorded using a BRUKER ALPHA spectrophotometer with a wavenumber range of 4000 ~ 400 cm^{-1} with a resolution of 2 cm^{-1}.

Gas Sorption

Fresh MFU-4l(Zn)-Cl/Br/I (ca. 40 mg) was prepared and the solvent was exchanged by Soxhlet extraction with methanol for approximately 48 hours. Then the samples were filtrated, and dried under vacuum overnight to get fully activated before gas sorption experiments. Subsequently, the samples were transferred in a pre-weighed analysis tube, and heated at 120 °C for 480 min to remove all residual solvent on Micromeritics ASAP 2020 adsorption analyser. The sample tube was re-weighed to obtain a consistent dry mass for the degassed sample. Gas sorption isotherms were recorded volumetrically at 77 K for N_2, and Brunauer-Emmett-Teller (BET) surface area data were calculated using N_2 adsorption data at 77 K in the relative pressure range of 0.01~0.1 P/P_0.

Thermogravimetric Analysis (TGA)

TGA analysis was carried out on a TGA Q5000 differential thermal analyzer. The samples were heating in N_2 stream from 25 to 800 °C with a heating rate of 10 °C min^{-1}.

Chemical and Thermal Stability Studies

~100 mg of the as-synthesized materials were incubated in various organic solvent (including DMF, EtOH, CH_2Cl_2) and DI water in air for 24 h. The samples were exposed into the above conditions for 24 h before performing PXRD and fluorescence measurements. Thermal stability experiments were carried out by as-synthesized MOFs in oven at 200, 250, 300 and 350 °C for 12 h. After cooling to the room temperature naturally, PXRD and fluorescence characterization were performed.

Scanning Electron Microscopy (SEM) images

Scanning electron microscopy (SEM) were performed on a table-top Pheom Pro instrument using a 10 kV energy source under vacuum.

Energy Dispersive X-ray Analysis (EDS)

Energy dispersive X-ray analysis (EDS) data and EDS mapping images were obtained at Hitachi S-4800 (Hitachi, Japan).

Photo Images

Photo images were collected using an HUAWEI HONOR 10 Smartphone under ambient light or under the irradiation of a 4W, 365 nm UV lamp.

Ultraviolet-Visible (UV-Vis) Diffuser Reflectance Spectrum

UV-visible diffuse reflectance spectroscopy was performed on Shimadzu UV-2600 UV-Vis spectrophotometer equipped with an integrating sphere, using 100% $BaSO_4$ as reflectance standard for all measurements.

Steady State Photoluminescence Spectra

The excitation and emission spectra of synthesized materials were measured on a Horiba Fluorolog setup in reflection geometry (FLUOROLOG-3C-111). The emission spectra were obtained under 365 nm excitation, using 1 nm scan step and 1.2 nm slit width.

Time-resolved Photoluminescence

Time-resolved emission data was collected at room temperature using steady state/transient

state fluorescence/phosphorescent spectrometer equipped with time-correlated single photon counting (TCSPC) system (FLUOROLOG-3-11). Excitation light with the specific wavelength was provided by an EPL-360PS pulsed diode laser. The average lifetime was calculated according to the following equation:

$$\tau_{avg} = \frac{\sum a_i \tau_i^2}{\sum a_i \tau_i} \quad i = 1, 2, 3, \cdots$$

where a_i represents the amplitude of each component and τ_i represents the decay time.

Temperature-Dependent Photoluminescence

Temperature-dependent emission data of $Zn_5Br_4BTDD_3$ was collected applying HORIBA FLUOROLOG-3C-111 steady state fluorescence spectrometer at a series of temperature ranged from 77 K to 378 K.

Photoluminescence Quantum Efficiency (PLQE)

Absolute PLQE measurements of synthesized materials were performed on an HORIBA FLUOROLOG-3C-111 steady state/transient state fluorescence/phosphorescent spectrometer with an integrating sphere ($BaSO_4$ coating) using single photon counting mode. The focal length of the monochromator was 300 mm. Samples were excited at 365 nm light output from a 450 W Xe lamp with 1 mm excitation slits width. Emission spectra of $Zn_5X_4BTDD_3$ were guided through a single grating Czerny-Turner monochromator and detected by a Hamamatsu R928P photomultiplier tube using a scan step of 0.2 nm, a scan dwell time of 0.2 s, and an emission slit width of 0.1 mm. The value of PLQYs were calculated according to the following equation: $\varphi = k_f/k_a$, in which k_f means the number of emitted photons and ka means the number of absorbed photons. Control sample, Rhadamine-101, was measured using the same method to give a PLQY of 95%, which is close to the literature value.

Photostability Tests

The photostability study of synthesized materials was measured by employing a 4W, 365 nm UV lamp as the continuous irradiation source in surrounding environment (~60% relative humidity, room temperature) for 7d to test their long-term photostability.

Raman Measurement

The solid-state Raman spectra were recorded on a CRIAC 20/30PV Technologies micro

spectrophotometer with a 514 nm excitation wavelength. Crystals were placed on quartz slides under Krytox oil, and data was collected after optimization of micro spectrophotometer.

Supporting Tables and Figures

Table S1. Photophysical properties of MFU-4l(Zn).

Material	λ_{abs} (nm)[a]	λ_{em} (nm)[b]	(x, y)[c]	PLQE (%)[d]
MFU-4l(Zn)-Cl	366	467	(0.22,0.27)	1.12
MFU-4l(Zn)-Br	364	466	(0.19,0.23)	3.20
MFU-4l(Zn)-I	362	431	(0.17,0.14)	0.79

[a]λ_{abs} is the absorption edge; [b]λ_{em} is the maximum emission wavelength; [c](x,y) is the Commission Internationale de l'Eclairage (CIE) chromatic coordinates; [d]PLQE is photoluminescence quantum efficiency.

Table S2. Photophysical properties of Alq3@MFU-4l(Zn)-Br.

Concentrations of Alq3[e]	λ_{em} (nm)	(x, y)	CCT (K)[f]	Lifetime (ns)[g]
1.7 wt%	467	(0.25,0.29)	12837	2.78
2.1 wt%	481	(0.26,0.32)	10798	3.01
2.5 wt%	505	(0.27,0.36)	8321	4.62

[e]Concentrations of Alq3 was determined by Inductively coupled plasma-optical emission spectroscopy (ICP-OES); [f]CCT is correlated color temperature; [g]PL lifetimes are excited at 340 nm.
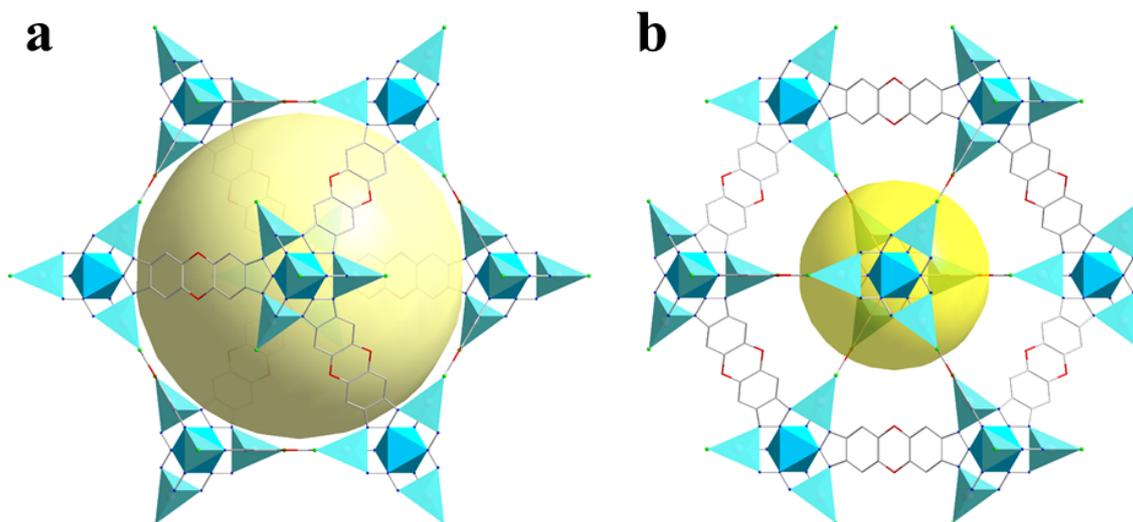
Figure S1. Crystallographic view of two cages in MFU-4l(Zn)-Cl, (a) Cage A (light yellow, 18.56 Å) and (b) Cage B (yellow, 11.97 Å) (viewing direction: h, k, l=1).   Zn turquoise, Cl green, N blue, O red, C grey.   Hydrogen atoms are omitted for clarity.
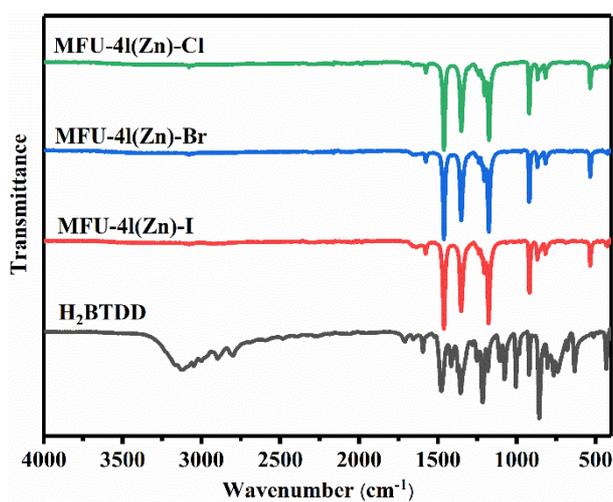
Figure S2. FTIR spectrum of synthesized MFU-4l(Zn)-Cl (green), MFU-4l(Zn)-Br (blue), MFU-4l(Zn)-I (red), and H_2BTDD (black).

a

5 μm

b

5 μm

c

4 μm
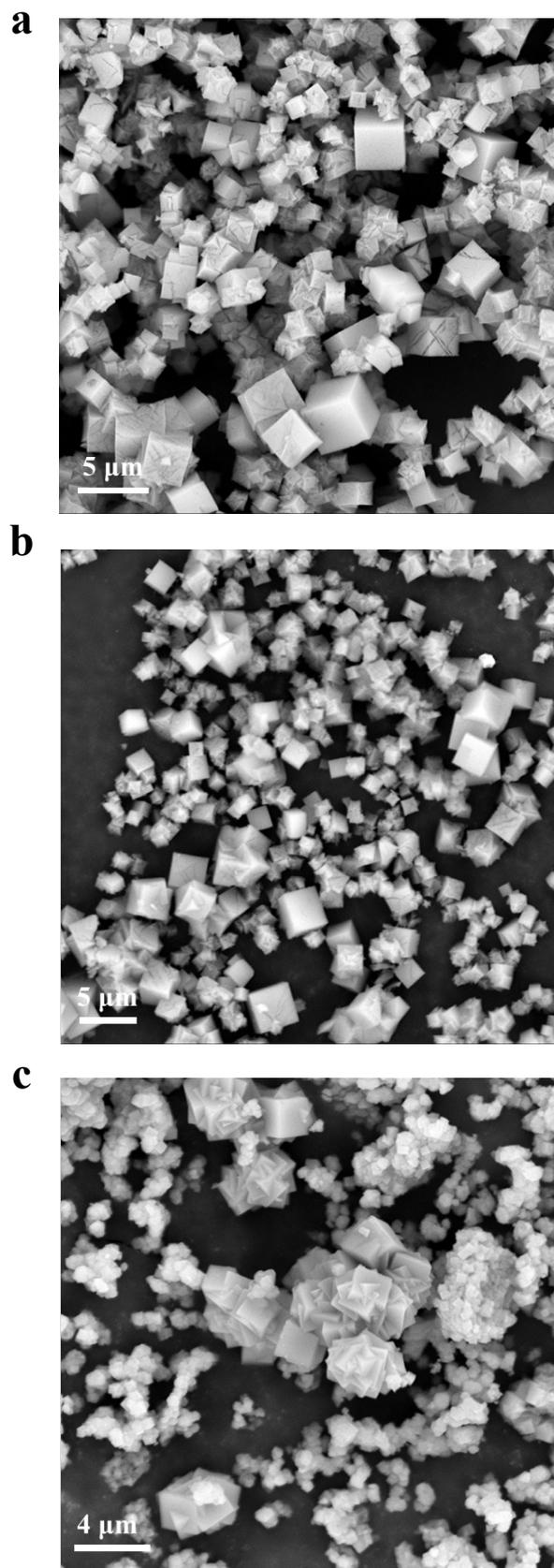
Figure S3. SEM images of (a) MFU-4l(Zn)-Cl, (b) MFU-4l(Zn)-Br, and (c) MFU-4l(Zn)-I.
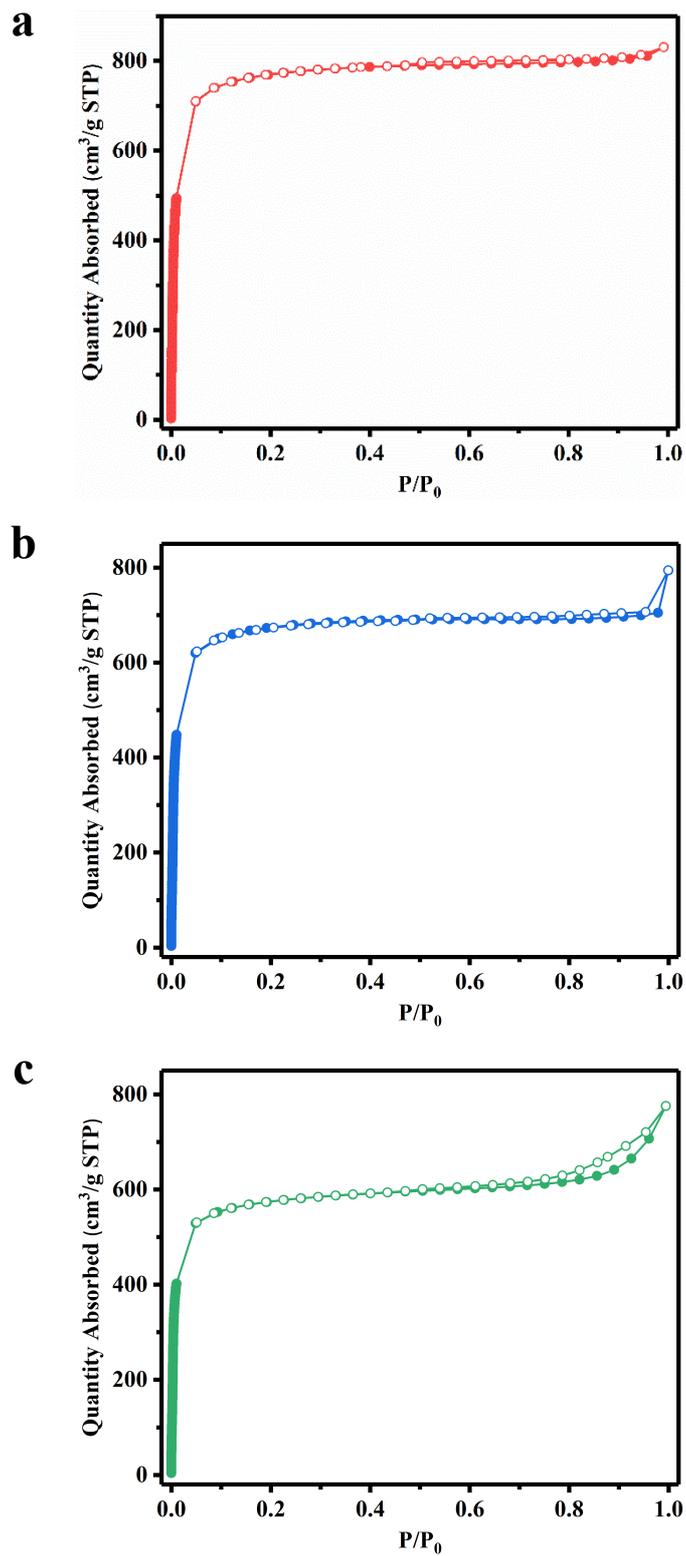
Figure S4. N$_2$ sorption at 77 K of activated (a) MFU-4l(Zn)-Cl, (b) MFU-4l(Zn)-Br, and (c) MFU-4l(Zn)-I.
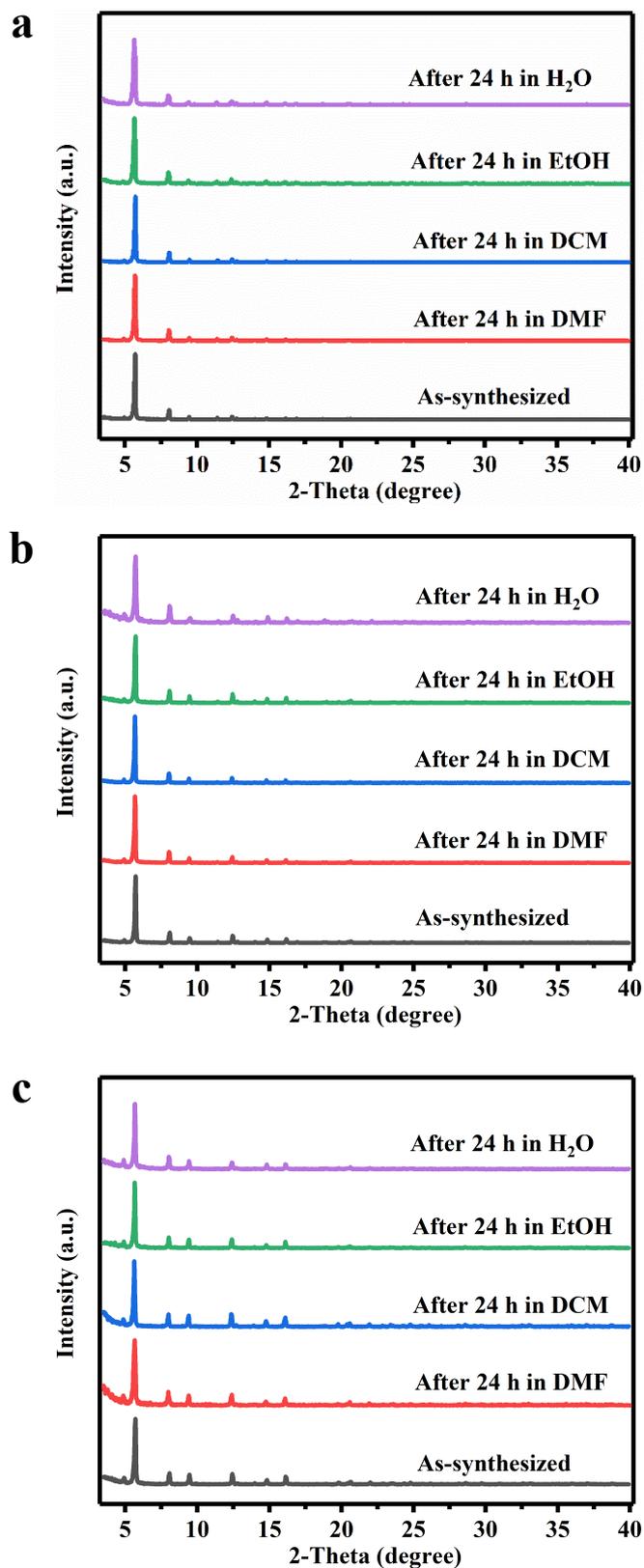
Figure S5. PXRD patterns of (a) MFU-4l(Zn)-Cl, (b) MFU-4l(Zn)-Br, and (c) MFU-4l(Zn)-I before and after incubation in different solvents for 24 h.
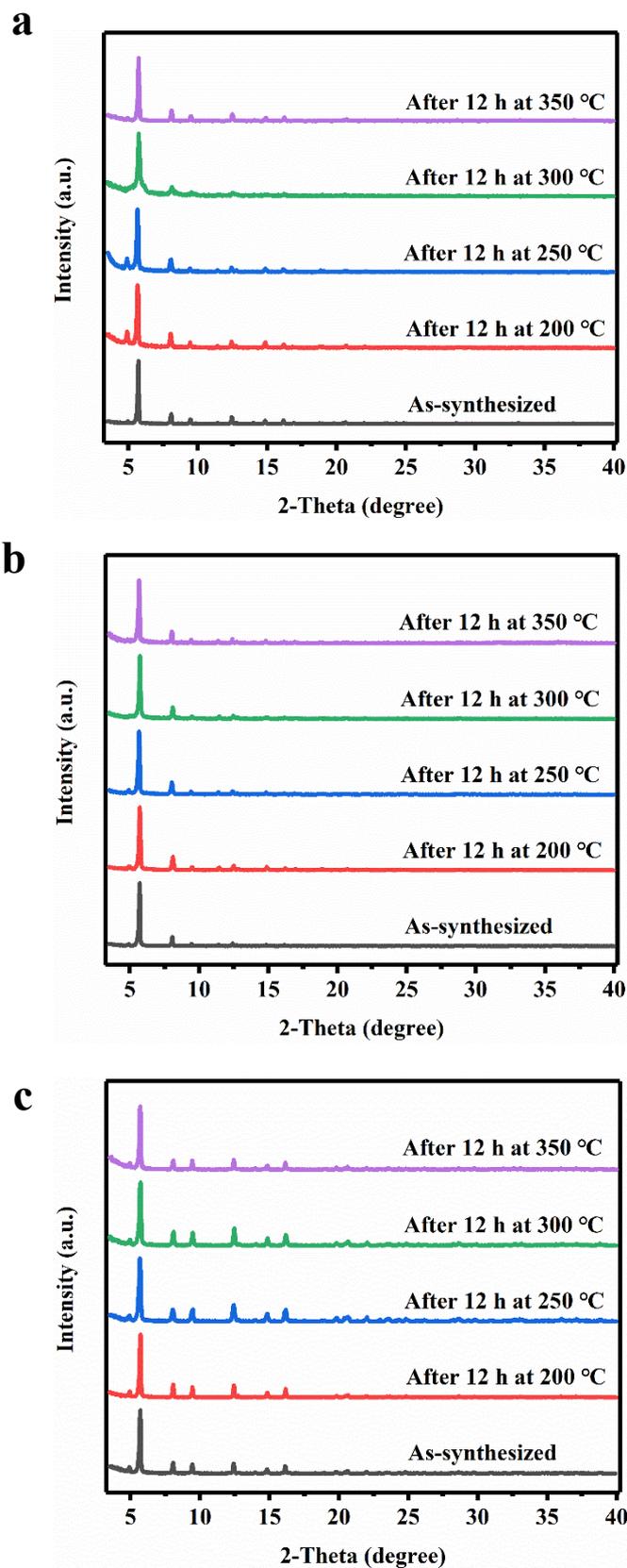
Figure S6. PXRD patterns of (a) MFU-4l(Zn)-Cl, (b) MFU-4l(Zn)-Br, and (c) MFU-4l(Zn)-I before and after thermal treatment in air for 12 h.
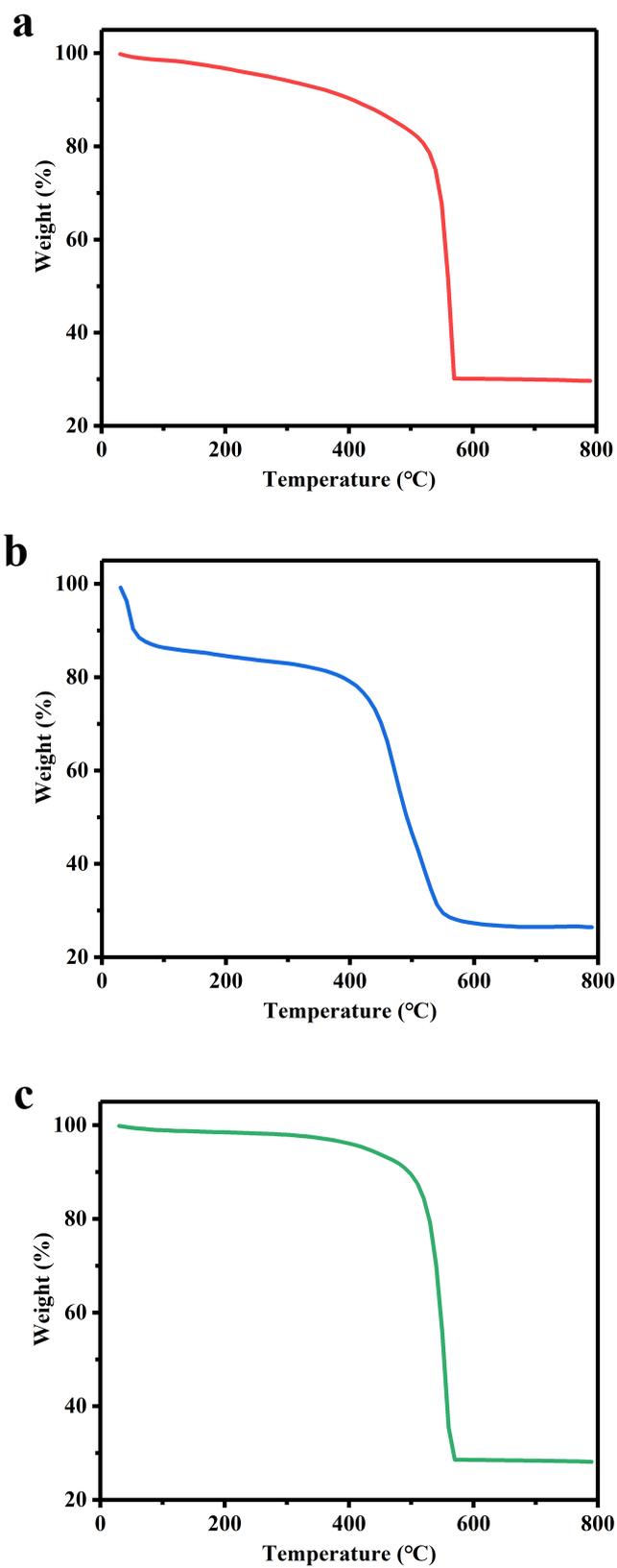
Figure S7. Thermogravimetric analysis of (a) MFU-4l(Zn)-Cl, (b) MFU-4l(Zn)-Br, and (c) MFU-4l(Zn)-I under N_2 flow.
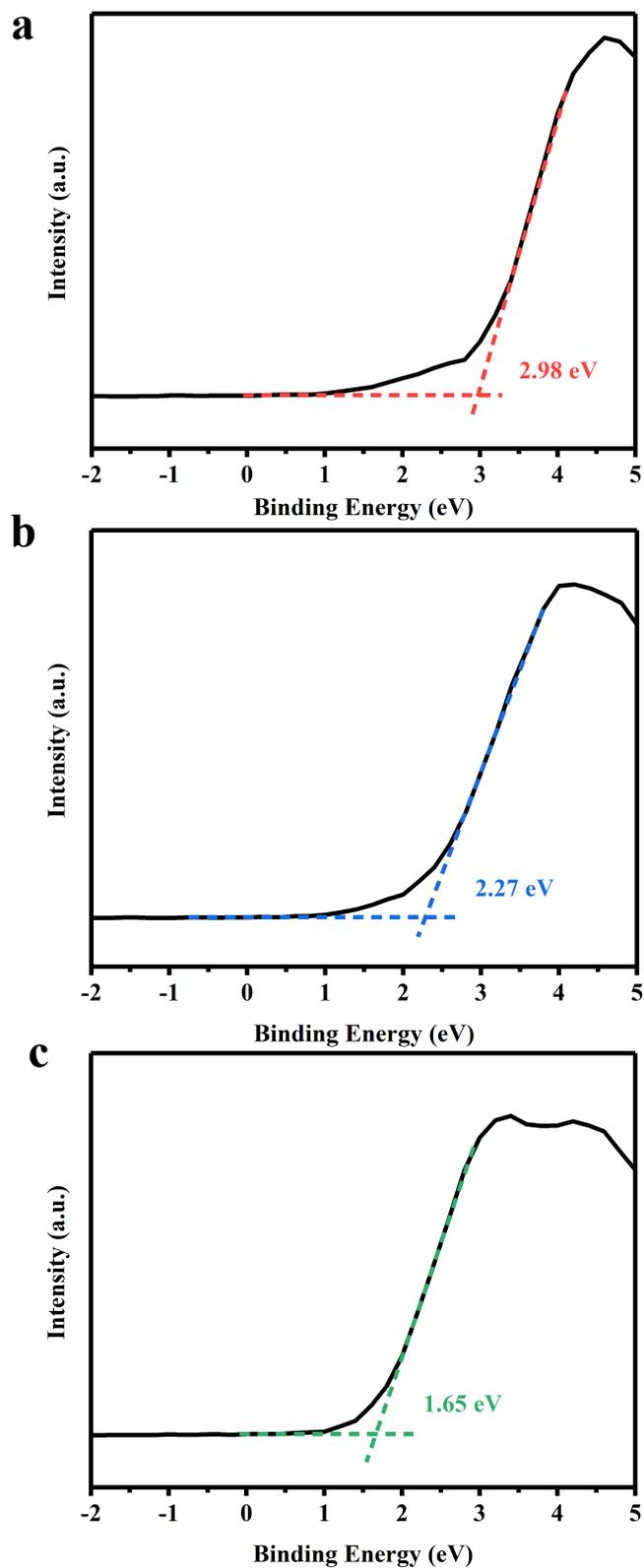
Figure S8. XPS valence band spectra of (a) MFU-4l(Zn)-Cl, (b) MFU-4l(Zn)-Br, and (c) MFU-4l(Zn)-I. The extrapolation of the linear region estimates the valence band value of ~2.98, ~2.27, and ~1.65 eV for (a) MFU-4l(Zn)-Cl, (b) MFU-4l(Zn)-Br, and (c) MFU-4l(Zn)-I, respectively.
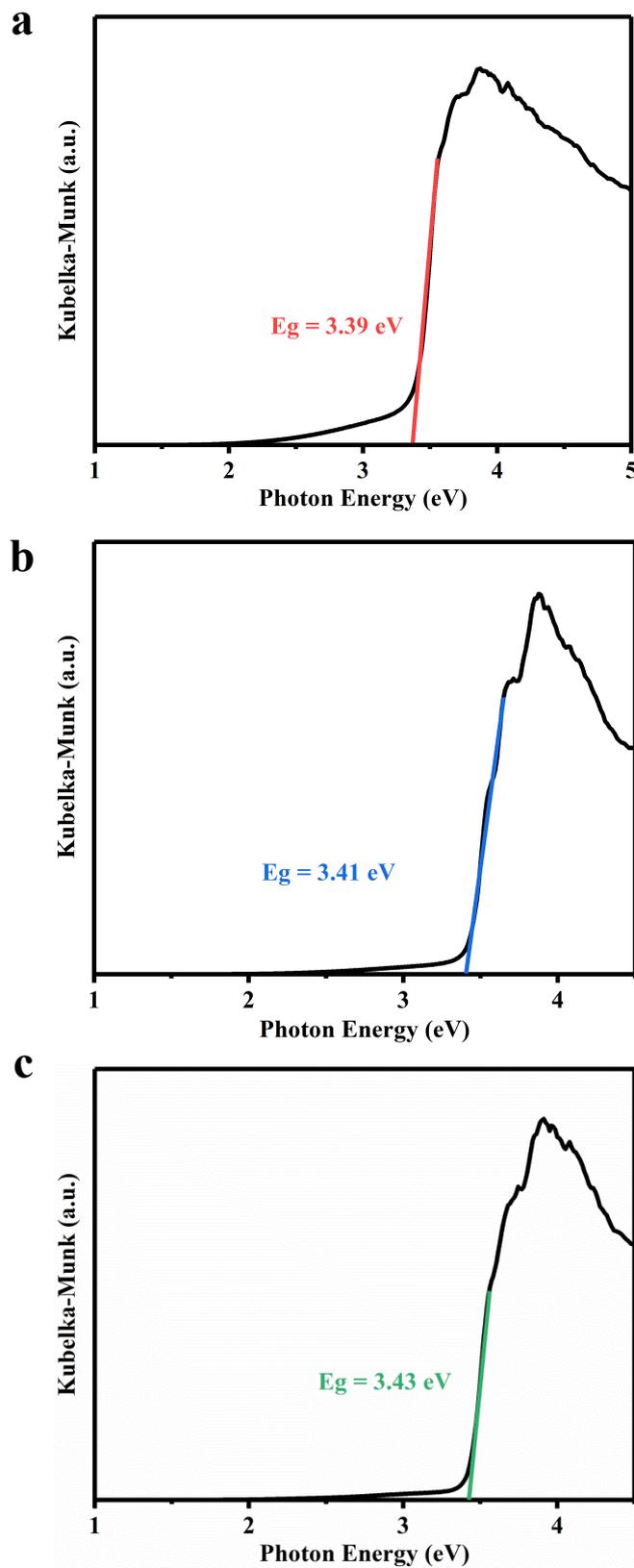
Figure S9. Kubelka-Munk plot of (a) MFU-4l(Zn)-Cl, (b) MFU-4l(Zn)-Br, and (c) MFU-4l(Zn)-I. The extrapolation of the linear region estimates the bandgap value of ~3.39, ~3.41, and ~3.43 eV for (a) MFU-4l(Zn)-Cl, (b) MFU-4l(Zn)-Br, and (c) MFU-4l(Zn)-I, respectively.
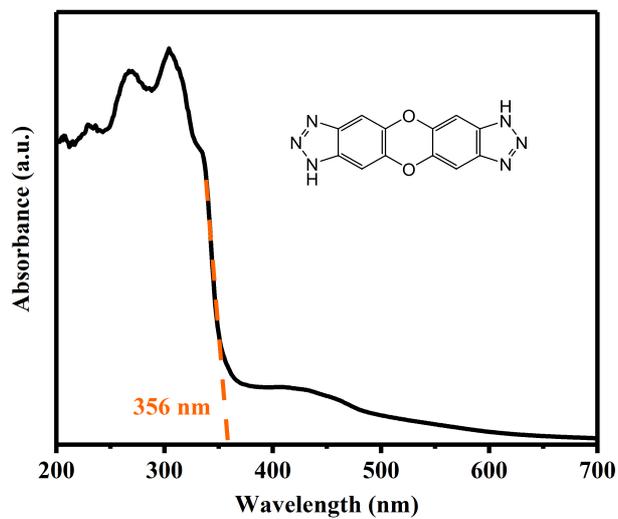
Figure S10. The absorption spectrum of the free H_2BTDD ligands, which has an absorption edge of 356 nm.
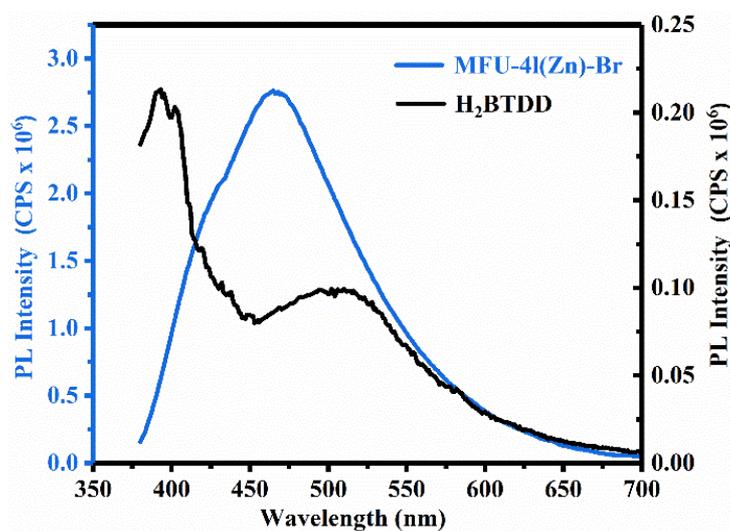
Figure S11. Room temperature emission spectra of MFU-4l(Zn)-Br and the free H_2BTDD ligands.
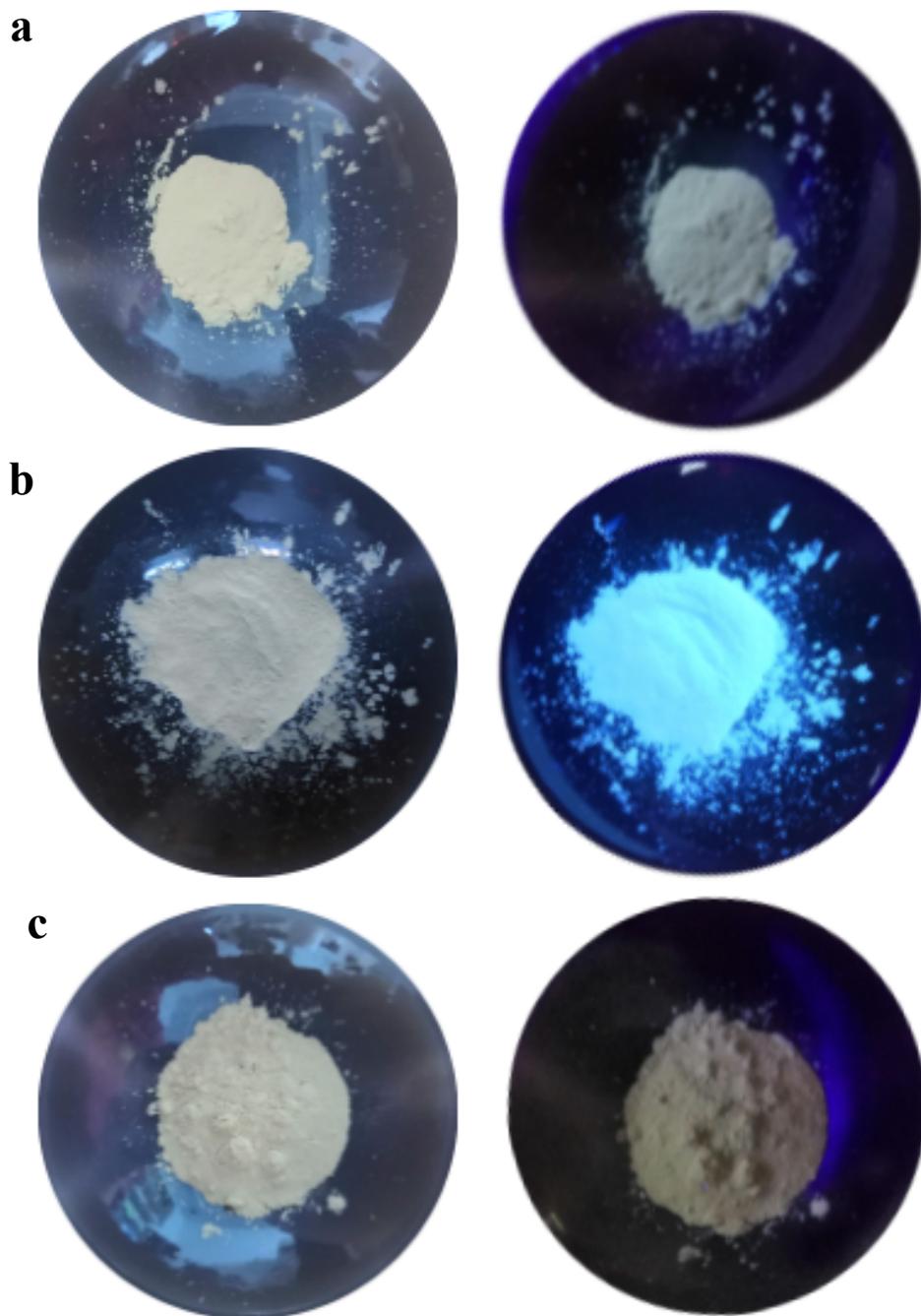
Figure S12. Photo images of (a) MFU-4l(Zn)-Cl, (b) MFU-4l(Zn)-Br, and (c) MFU-4l(Zn)-I under ambient daylight (left) and under the irradiation of a 4 W, 365 nm UV lamp (right).
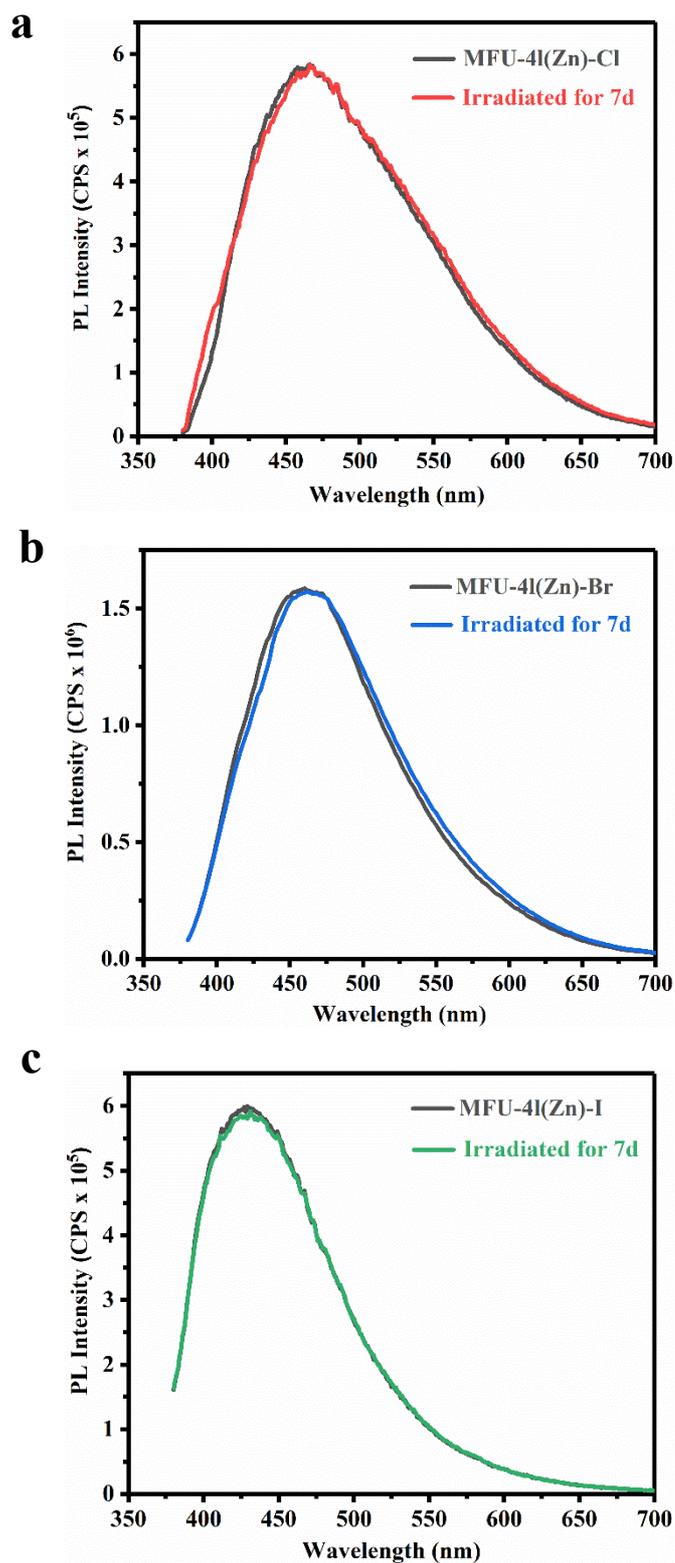
Figure S13. Room temperature emission spectra of (a) MFU-4l(Zn)-Cl, (b) MFU-4l(Zn)-Br, and (c) MFU-4l(Zn)-I after irradiation (4 W, 365 nm UV-lamp) for 7 days in air (~ 60% RH, room temperature).
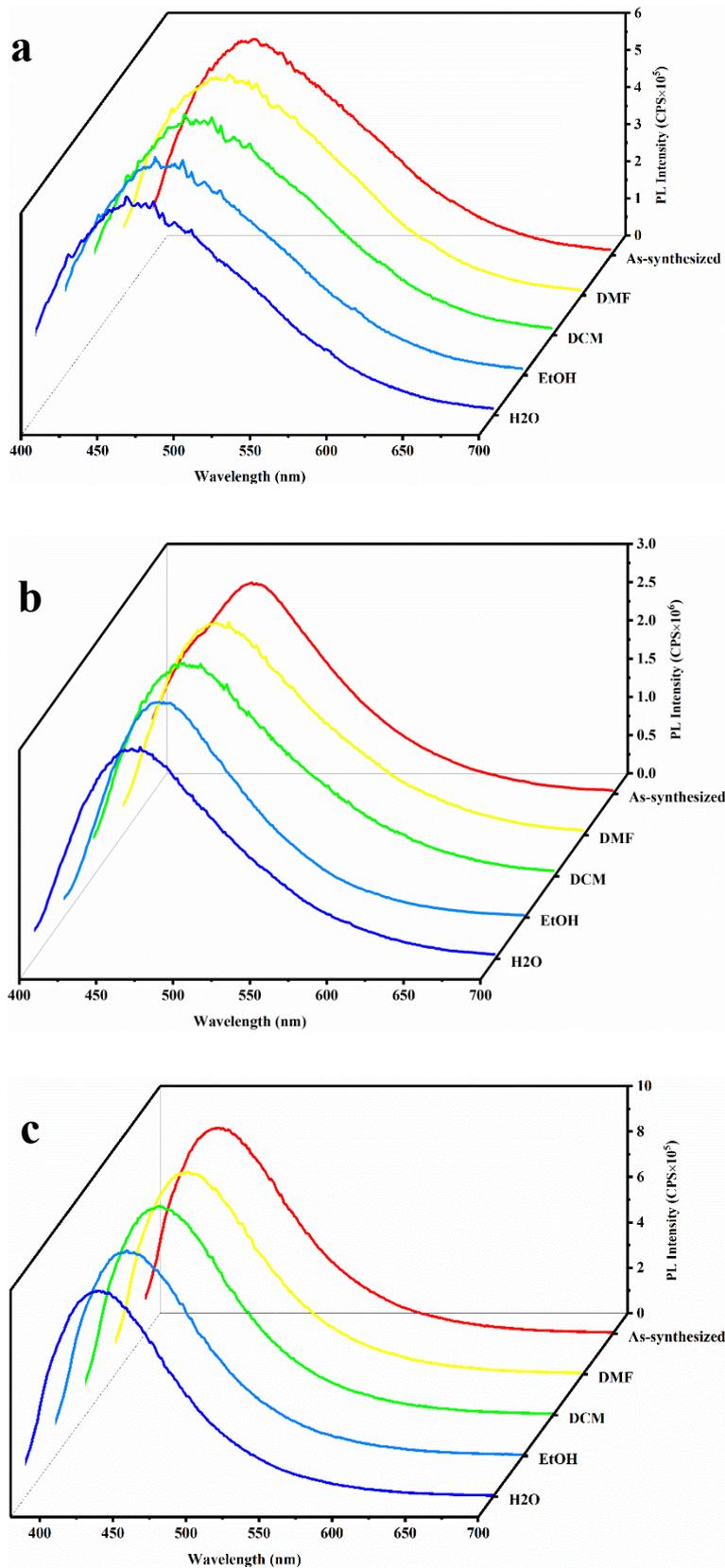
Figure S14. Room temperature emission spectra of (a) MFU-4l(Zn)-Cl, (b) MFU-4l(Zn)-Br, and (c) MFU-4l(Zn)-I before and after incubation in different solvents for 24 h.
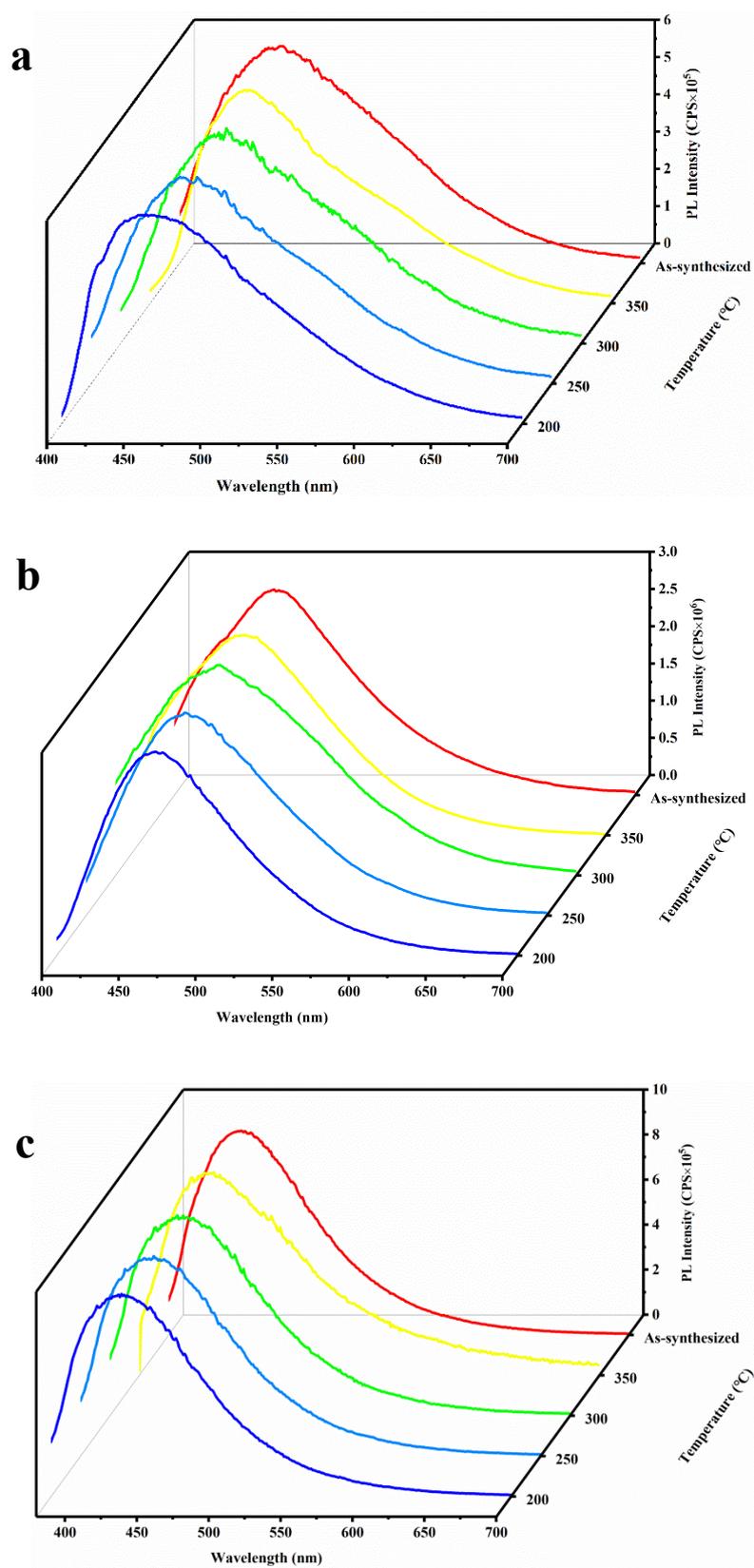
Figure S15. Room temperature emission spectra of (a) MFU-4l(Zn)-Cl, (b) MFU-4l(Zn)-Br, and (c) MFU-4l(Zn)-I before and after thermal treatment in air for 12 h.
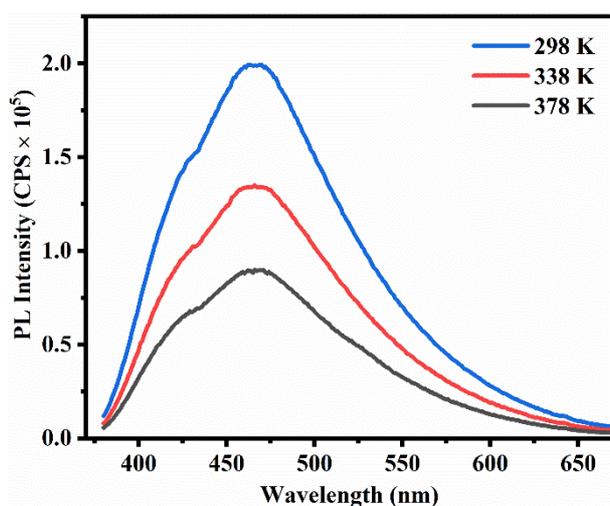
Figure S16. Emission spectra of MFU-4l(Zn)-Br at 298, 338, and 378 K. The thermal quenching phenomenon is largely induced by an increased level of non-radiative recombination (indirect recombination) with temperature increasing.
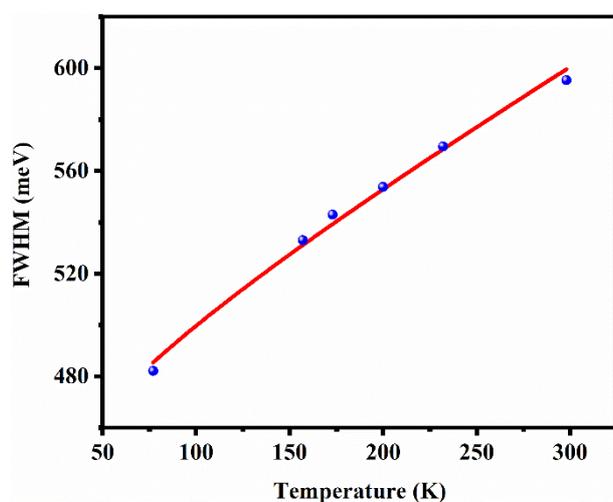
Figure S17. Temperature-dependent FWHM of the emission band in MFU-4l(Zn)-Br (blue symbols) and the best fit to eq. 1 in the manuscript (red line). A fit to the data gives Γ_0= 439(1) meV, Γ_{LO} = 126(7) meV, Γ_{inh} = 107(6) meV, E_{LO} = 25(3) meV, E_b = 6(1) meV, where Γ_0 represents the emission FWHM at $T = 0$ K, E_{LO} is the energy of the longitudinal optical phonon energy, and E_b represents the average binding energy of the impurity exciton complexes. Γ_{LO} and Γ_{inh} give the relative contributions of exciton-phonon coupling and inhomogeneous broadening (induced by trap states), respectively.
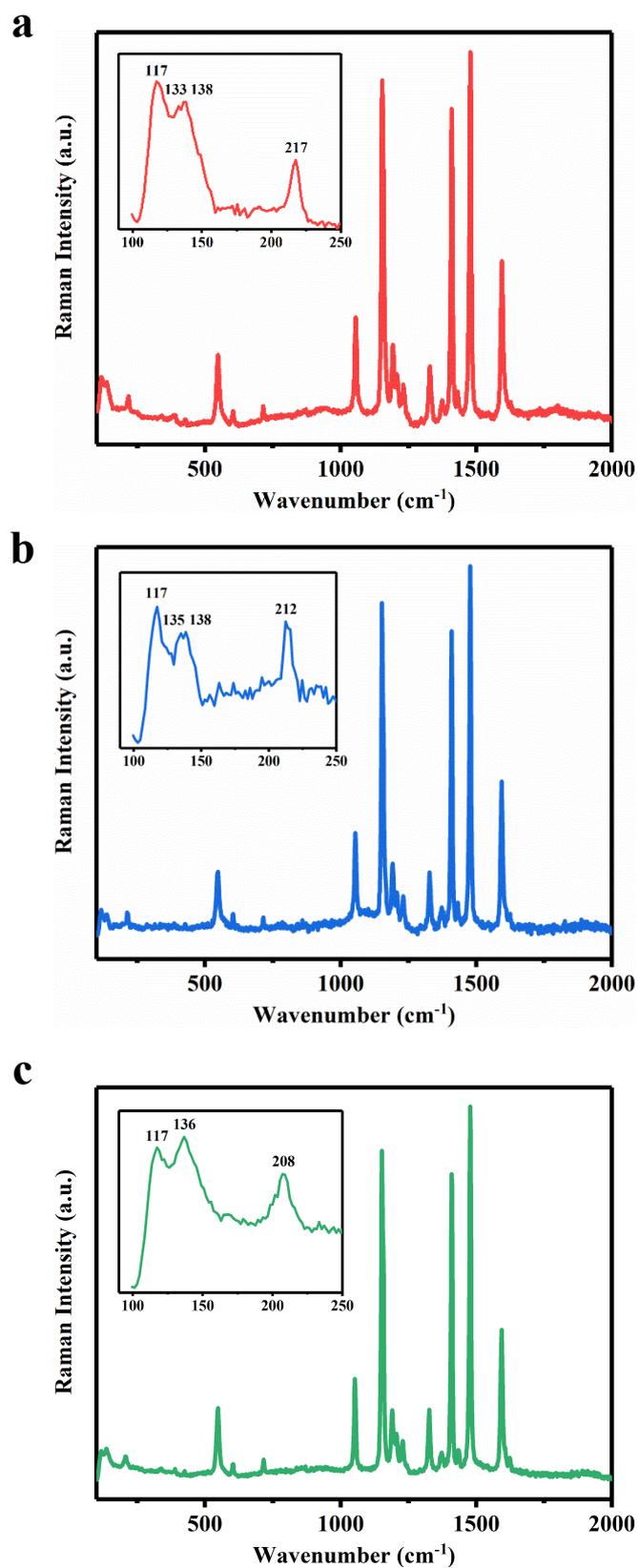
Figure S18. Raman spectra of (a) MFU-4l(Zn)-Cl, (b) MFU-4l(Zn)-Br, and (c) MFU-4l(Zn)-I.
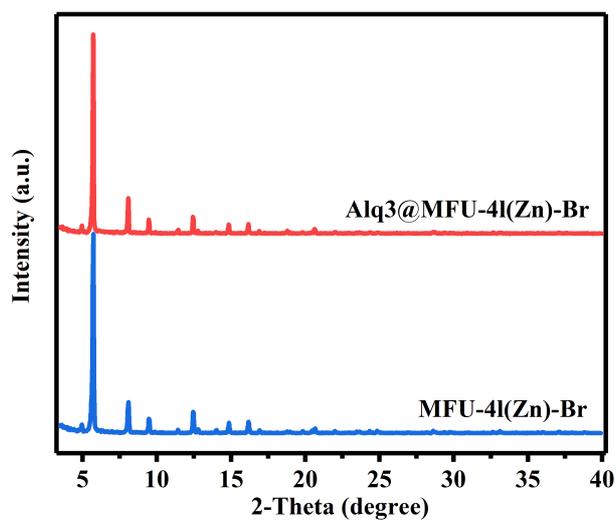
Figure S19. PXRD patterns of synthesized MFU-4l(Zn)-Br (blue) and 2.5 wt% Alq3@MFU-4l(Zn)-Br (red).
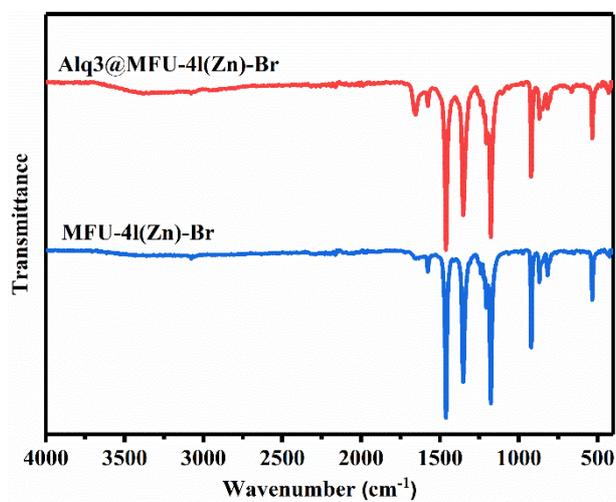
Figure S20. FTIR spectrum for synthesized MFU-4l(Zn)-Br (blue) and 2.5 wt% Alq3@MFU-4l(Zn)-Br (red).
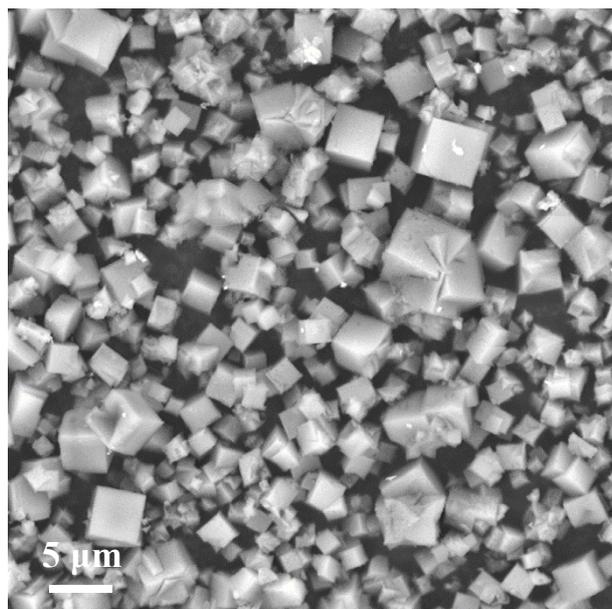
Figure S21. SEM images of 2.5 wt% Alq3@MFU-4l(Zn)-Br.
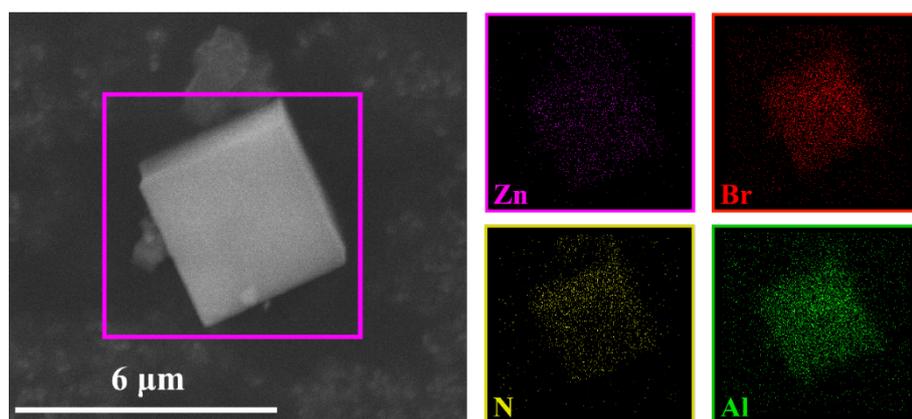
Figure S22. EDS elemental mapping of 2.5 wt% Alq3@MFU-4l(Zn)-Br.
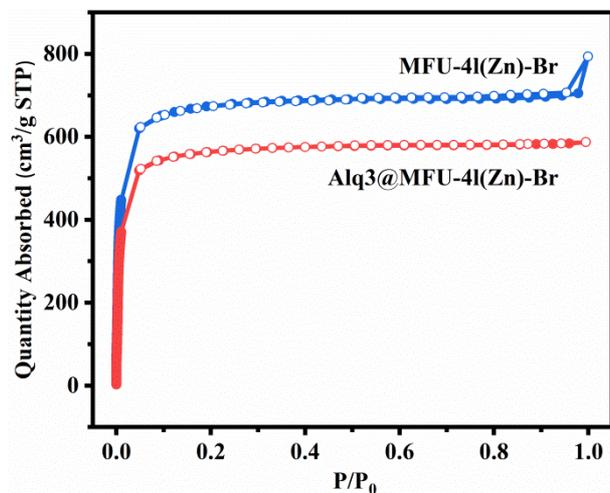
Figure S23. N$_2$ sorption at 77 K of activated MFU-4l(Zn)-Br (blue) and 2.5 wt% Alq3@ MFU-4l(Zn)-Br (red).
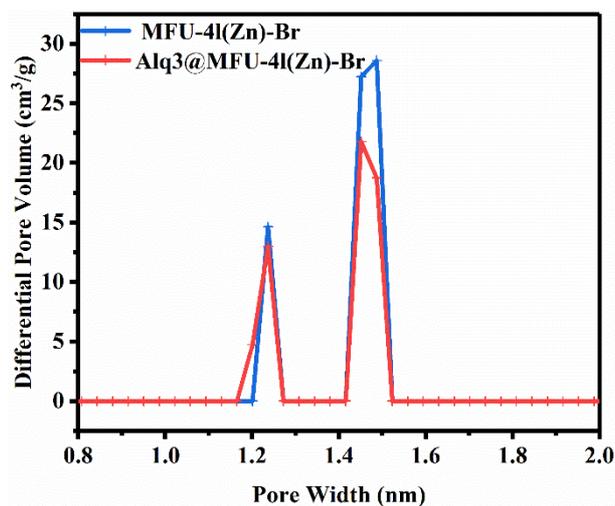
Figure S24. Pore width distribution of MFU-4l(Zn)-Br (blue) and 2.5 wt% Alq3@MFU-4l(Zn)-Br (red).
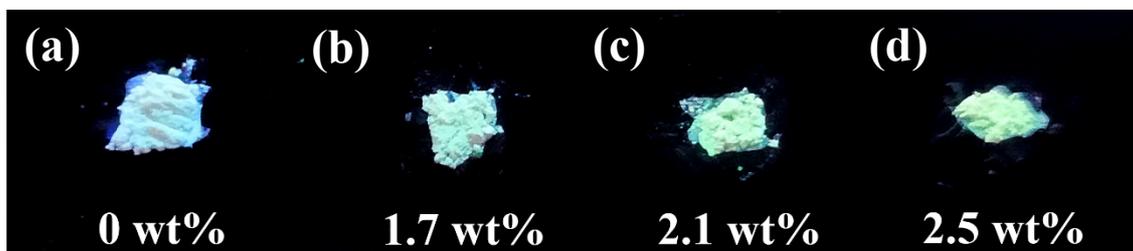
Figure S25. Photo images of 0 wt%, 1.7 wt%, 2.1 wt%, and 2.5 wt%@Alq3@MFU-4l(Zn)-Br upon the irradiation from a 4W, 365 nm UV lamp.
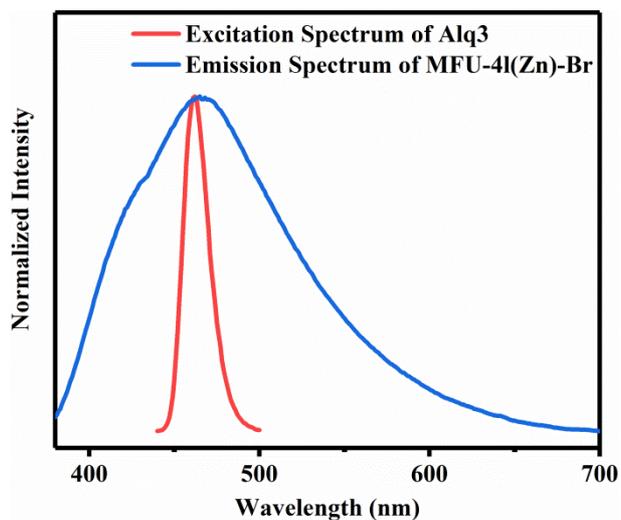
Figure S26. The excitation spectrum of Alq3 and emission spectrum of MFU-4l(Zn)-Br.
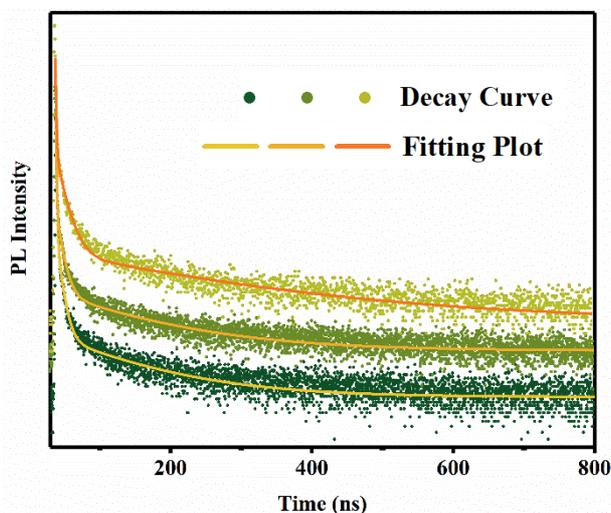
Figure S27. PL decay curve and fitting plot of (a) 1.7 wt% Alq3@MFU-4l(Zn)-Br (bottom, dark green), (b) 2.1 wt% Alq3@MFU-4l(Zn)-Br (middle, green), and (c) 2.5 wt% Alq3@MFU-4l(Zn)-Br (top, yellow green). The fitting plots estimate the PL lifetimes are 2.78, 3.01, and 4.62 ns for 1.7 wt% Alq3@MFU-4l(Zn)-Br, 2.1 wt% Alq3@MFU-4l(Zn)-Br, and 2.5 wt% Alq3@MFU-4l(Zn)-Br, respectively (Table S2). The y axis is logarithm of the photons numbers.

References

S1. A. J. Rieth, A. M. Wright, G. Skorupskii, J. L. Mancuso, C. H. Hendon, and M. Dincă, *J. Am. Chem. Soc.*, 2019, **141,** 13858-13866.

S2. D. Denysenko, M. Grzywa, M. Tonigold, B. Streppel, I. Krkljus, M. Hirscher, E. Mugnaioli, U. Kolb, J. Hanss, and D. Volkmer, *Chem. Eur. J.*, 2011, **17,** 1837-1848.